

Structural and Optical Properties of Zinc Oxide Nanoparticles Synthesized Using Continuous Spray Pyrolysis Reactor

V. Dutta, Venkata Phanikiran B. and Charu Dwivedi

Photovoltaic Laboratory, Centre for Energy Studies, Indian Institute of Technology Delhi,
Hauz Khas, New Delhi-110016, India, vducta@ces.iitd.ac.in

ABSTRACT

ZnO nanoparticles were prepared by injecting atomized droplets of spray solution containing zinc precursor into a heated reactor. Structural properties of ZnO nanoparticles thus created were investigated using X-ray diffraction (XRD) and transmission electron microscopy (TEM). The TEM picture showed nearly monodispersed ZnO nanoparticles having average particle size ~ 25 & 18 nm as collected from different outlets. The X-ray diffraction (XRD) gave pure ZnO peaks. The PL spectra indicated the presence of oxygen related defect states. Monodispersed ZnO nanoparticles can thus be prepared on a continuous basis and used for making large area devices like Dye Sensitized Solar Cells (DSSC) and hybrid organic solar cells.

Keywords: Zinc Oxide, Spray pyrolysis, X-ray diffraction, Photoluminescence, Crystal structure

1 INTRODUCTION

Zinc oxide (ZnO) is a wide band gap, n-type semiconductor and is being extensively investigated due to its applications in devices such as Solar cells, UV photonics, transparent high-power electronics, varistors, surface acoustic wave devices, piezoelectric transducers and gas sensing devices [1-5]. The properties of ZnO strongly depend on their dimensions and morphologies [6]. Therefore, the preparation of ZnO nanoparticles/nanostructures is of critical importance for the development of novel devices [7].

Dye sensitized solar cell (DSSC) utilizes an oxide photoelectrode (TiO_2 , ZnO etc.) having nanopores for efficient dye adsorption and electron injection. The oxide nanoparticles can be suitably coated on a conducting glass substrate using techniques like spin coating, screen printing and spray deposition. Nanostructured ZnO photoelectrode has been used for improved DSSC performance. Rangarao et.al. showed that ZnO cell has an efficiency of $\sim 2.8\%$ for nanoparticle film and 4.7% for nanorod morphology film [8]. The increase in the efficiency is due to increase in the amount of dye adsorption for the nanorod morphology film.

Recently, it has been shown that ultra-fast photoinduced charge transfer can occur between a conjugated polymer and metal oxides [9,10]. In bulk (or dispersed) heterojunctions, ZnO nanoparticles are blend

into the polymer MEH-PPV [11], P3HT [12] and MDMO-PPV [13] to create a heterogeneous composite with a high interface surface area. This hybrid layer is used in organic solar cells.

A variety of techniques have been used to fabricate ZnO nanoparticles, which mostly yield small quantities of nanoparticles. But for large area devices like DSSCs and organic solar cells, there is a requirement for nanoparticles in large quantities. Keeping this in view a spray pyrolysis reactor has been fabricated for continuous nanoparticle production.

Compared to other techniques, spray pyrolysis offers the possibility of preparing nanoparticles at low cost which can then be scaled up for industrial applications. The properties can be easily controlled over a wide range by changing the spray parameters, thus eliminating major drawbacks of chemical methods. The atomization can be effected using Ultrasonic Generator (USP) [14-16] or pressurized gas (SP).

In the spray pyrolysis route, chemical reactions proceed inside submicron liquid droplets of a (high boiling point) solvent in a heated inert/reactive gas stream; each liquid droplet is an individual phase-separated reactor. Hence, we can have the control over the product in terms of size, shape and stoichiometry by suitably controlling the physical and chemical parameters during the process. This kind of physical control is somewhat restricted in USP compared to SP route. In the later case, the equipment requirement is also simplified and therefore, we have designed a continuous spray pyrolysis reactor for the SP route. The details of the preparation technique are being patented [17] and only the properties of ZnO nanoparticles are reported.

2 EXPERIMENTAL DETAILS

ZnO nanoparticles were prepared using zinc precursor solution and various spray parameters such as flow rate, gas pressure, reactor temperature etc. were varied to obtain the nanoparticles [18]. The nanoparticles were collected from multiple outlets in different round bottom flasks. Phillips CM12 120KV transmission microscope is used for TEM studies. XRD studies are done using X-ray diffractometer (Phillips X'PERT PRO). 200kV Technai G20- high-resolution transmission electron microscope is used for HRTEM studies. PL spectra are recorded using a Perkin-Elmer Spectrometer (model: LS 55). A Xenon lamp is used to select the wavelength (300nm for this case) for exciting the sample to record the excitation spectra.

3 RESULTS AND DISCUSSIONS

3.1 Structural Studies

The TEM images in Fig. 1 shows that nearly monodispersed nanoparticles are collected from two outlets in the same experiment. Fig. 1(a) corresponds to the outlet at the centre and Fig. 1(b) corresponds to the one away from the centre. The outlets will be referred to as O-1 and O-2, respectively. The nanoparticles of average size ~ 25 nm are collected at O-1 (Fig.1(c)), whereas the ones collected from O-2 are found to be finer particles (~ 18 nm) (Fig.1(d)). This clearly indicates that differently sized nanoparticles can be separately collected in this technique.

It can be seen that there is a change in the average particle size which can occur due to the change in droplet sizes across the cross sectional area of the reactor. It seems that the bigger droplets are formed closer to the central region and smaller droplets are formed away from the centre. Since the collection is done at a selected region, most nanoparticles are of nearly equal size. Thus, the technique can yield nanoparticles of different sizes with the possibility of collecting nearly equal sized particles, depending on the outlet position.

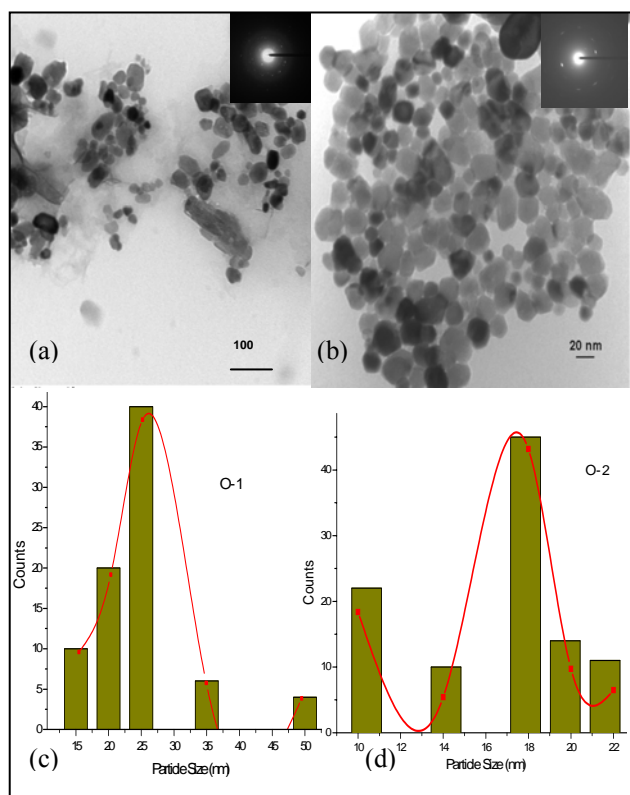


Fig. 1 TEM images of ZnO nanoparticles as collected from the outlets (a) O-1 and (b) O-2 in the same experiment. The particle size distributions are shown in Fig. 1(c) and 1(d)

Also, the Selected Area Diffraction (SAD) pattern shows the diffraction rings corresponding to the lattice planes of ZnO confirming the crystalline nature of the ZnO nanoparticles.

The HRTEM image (Fig. 2) also shows the lattice resolution having the d-spacing in the range 0.25- 0.27 nm which corresponds to (100) crystal. The particle size is close to 18 nm.

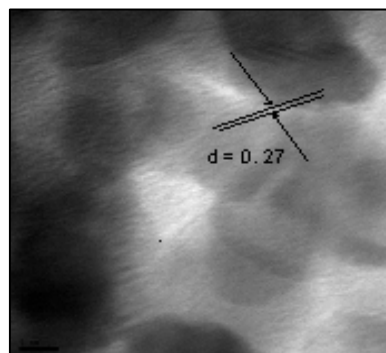


Fig. 2 HRTEM image of ZnO nanoparticles

The XRD pattern for ZnO nanoparticles at O-1 and O-2 are given in Fig. 3(a) and 3(b), respectively.

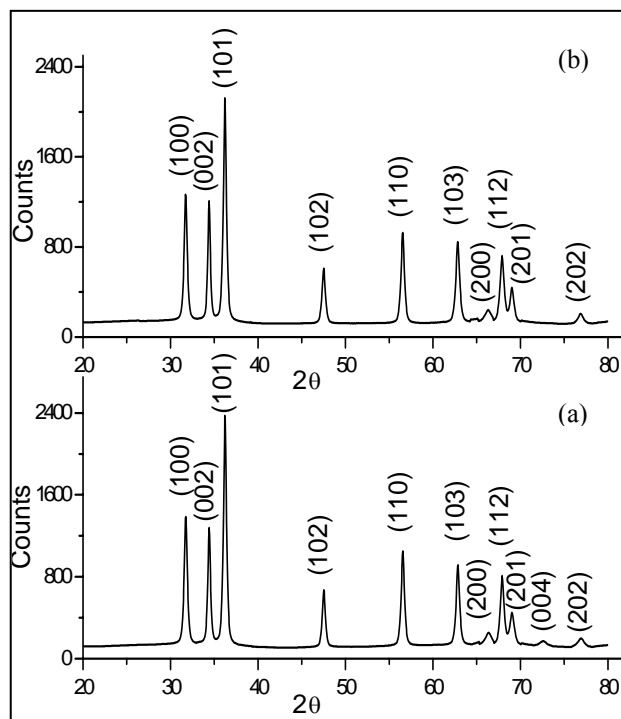


Fig. 3 X-ray diffractogram of ZnO nanoparticles collected from (a) O-1 and (b) O-2.

ZnO peaks that are matching with the JCPDS data files are obtained. The only difference is that the (004) peak is

missing in Fig. 3(b). The X-ray diffractogram confirms the hexagonal structure for ZnO nanoparticles which is in good agreement with the SAD pattern.

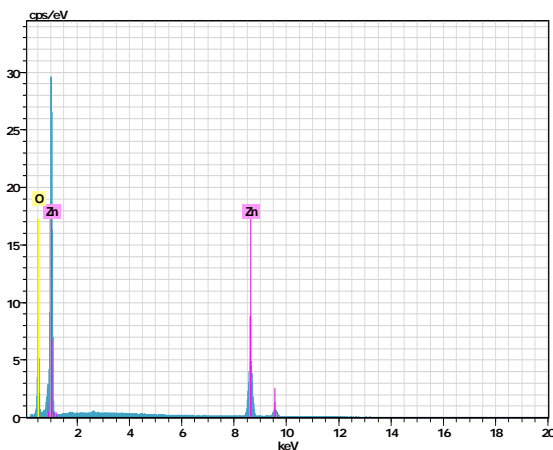
The grain size can be calculated using the Scherrer formula:

$$D = (0.9 \lambda) / (B \cos \theta) \quad (1)$$

where, D , λ , θ and B are the mean grain size, the X-ray wavelength of 0.154 nm, Bragg diffraction angle and the FWHM of the diffraction peak of the (h k l) direction at around $(2\theta)^\circ$ for ZnO nanoparticles, respectively. For the (1 0 1) peak the mean grain size values are found to be about 20 nm & 18 nm for O-1 and O-2, respectively, which are close to the TEM pictures particle size values.

3.2 EDX Studies

The EDX spectrum (Fig.4) shows the compositional analysis of Zn and O in atomic percent.



S.No.	OUTLET	Zn (At.%)	O (At.%)
1.	O- 1	39	57
2.	O- 2	44	55

Fig. 4 EDX spectra of ZnO nanoparticles and the corresponding stoichiometry.

Apparently, the droplet size difference does not only leads to the different nanoparticle sizes. But the stoichiometric changes are also occurring due to the different rates of the chemical and physical reactions, which depend on the droplet size, taking place inside the reactor.

Stoichiometrically, 65.38 gm of Zn reacts with 16 gm of oxygen to form 81.38 gm of ZnO. Hence, 1 gm of Zn reacts with 0.24 gm of O₂ to form 1.12 gm of ZnO. Ideally assuming that x gm of Zn present in the precursor has been converted to ZnO, the total collection is supposed to be about 1.12 x gm. But the total collection is about 0.68x gm, nevertheless this is a good amount of collection.

3.3 Photoluminescence Studies

The room temperature PL spectra of the samples collected from O-1 and O-2 are plotted in Figure 5. Three strong peaks at ~ 420, 480 and ~ 526 nm can be observed. Since the samples are oxygen rich, as is clear from EDX data (Fig. 4), the emissions can be attributed to excess oxygen related defects [19].

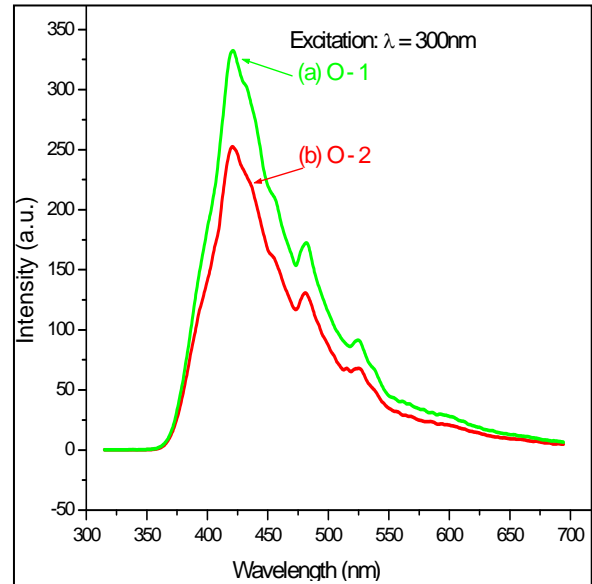


Fig. 5 Photoluminescence spectra of ZnO nanoparticles as collected from (a) O-1 and (b) O-2.

A change in the peak intensity of the nanoparticles collected from separate outlets and a slight hump at 3.1 eV corresponding to 390nm wavelength can also be seen. The mechanism of the 2.9eV (corresponding to 390nm) luminescence is not understood, although there are suggestions that it may be associated with oxygen vacancies or Zn interstitials [20-23].

The PL results are in confirmation with the TEM results in that the particles collected from O-1 are bigger in size and hence can be giving a higher intensity in the photoluminescence spectra.

4 CONCLUSIONS

ZnO nanoparticles were prepared by using spray pyrolysis technique using zinc precursor solution. The TEM pictures showed nearly monodispersed ZnO nanoparticles having average particle size ~ 25 & 18 nm as collected from different outlets in the same experiment.

The X-ray diffraction (XRD) indicated pure ZnO peaks matching with that of the hexagonal ZnO nanoparticles. The PL analysis gave peaks corresponding to oxygen related defects, which confirms the oxygen rich nature of

the nanoparticles. EDX measurements also showed the same results.

Our studies show that the technique is suitable for preparation of pure ZnO nanoparticles of nearly equal size and stoichiometry. The possibility of doing a continuous operation will have a great potential in developing nanoparticles for large area devices like Dye Sensitized Solar Cells and hybrid organic solar cells.

There is a complete control over the system to synthesize the desired products. It is found that the particle size produced by spray pyrolysis has a narrow distribution and is controllable, and the purity of product is. Therefore, this confirms the versatility of the methodology.

REFERENCES

- [1] B. O'Regan, M. Gratzel, *Nature* 353, 737, 1991.
- [2] K. Ernst, M.C. Lux-Steiner, R. Kfnerkamp, in: H. Scheer, B. McNelis, W. Palz, H.A. Ossenbrink, P. Helm (Eds.), *Proceedings 16th European Photovoltaic Solar Energy Conference*, Glasgow, U.K., May 1–5, 2000, p.63.
- [3] A. Luque, A. Martí, *Phys. Rev. Lett.* 78, 5014, 1997.
- [4] H.W. Deckman, C.R. Wronski, H. Witzke, E. Yablonovitch, *Appl. Phys. Lett.* 42, 968, 1983.
- [5] H. Zhang and M. T. Swihart, *Chem. Mater.* 19, 1290, 2007.
- [6] C. Y. Zhang, *Physica B* 404, 138, 2009.
- [7] L. Schmidt-Mende and J. L. MacManus-Driscoll, *Materials Today* 10, 40, 2007.
- [8] A Ranga Rao and V Dutta, *Nanotechnology* 19, 445712, 2008.
- [9] P. A. van Hal, M. M. Wienk, J. M. Kroon, W. J. H. Verhees, L.H. Sloof, W.J.H. van Genniip, P. Jonkheijm and R. A. J. Janssen, *Adv. Mater.* 15, 118, 2003.
- [10] A.J. Mozer, N.S. Saricitfi, L. Lusten, D. Vanderzande, R. Osterbacka, M. Westerling and G. Juska, *Appl. Phys. Lett.* 86, 112, 2005.
- [11] L. Yuan, Z.P. Guo, K. Konstantinov, J.Z. Wang, H.K. Liu, *Electrochimica Acta* 51, 3680, 2006.
- [12] W. Bai, K.L. Choy, N.H.J. Stelzer, J. Schoonman, *Solid State Ionics* 116, 225, 1999.
- [13] W. Lenggoro, B. Xia, H Mizushima, K. Okuyama, N. Kijima, *Materials Letters* 50, 92, 2001.
- [14] K. Liu, B. F. Yang, H. Yan, Z. Fu, M. Wen, Y. Chen and J. Zuo, *Applied Surface Science* 255, 2052, 2008.
- [15] P. Singh, A. Kumar, Deepak and D. Kaur, *Optical Materials* 30, 1316, 2008.
- [16] M. T. Swihart, *Current Opinion in Colloid and Interface Science* 8, 127, 2003.
- [17] V. Dutta and V. Phanikiran B., "Design of Externally Controlled Fabrication System." (For Patent).
- [18] V. Dutta, V. Phanikiran B. and C. Dwivedi, *Handbook 18th International Photovoltaic Science and Engineering Conference & Exhibition*, Kolkata, India, Jan 19-23, p.396, 2009.
- [19] C. Chandrinou, N. Boukos, C. Stogios and A. Travlos, *Microelectronics Journal* 40, 296, 2009.
- [20] S. A. Studenikin, N. Golego, M. Cocivera, *J. Appl. Phys.* 84, 2287, 1998.
- [21] G. Xiong, U. Pal, J. G. Serrano, K. B. Ucer and R. T. Williams, *phys. stat. sol. (c)* 3, 3577, 2006.
- [22] D. H. Liu, L. Liao, J. C. Li, H. X. Guo, and Q. Fu, *Mater. Sci. Eng. B* 121, 77, 2005.
- [23] K. Vanheusden, W. L. Warren, C. H. Seager, B. E. Gnade, D. R. Tallant, and J. A. Voigt, *J. Appl. Phys.* 79, 7983, 1996.